Letter

Tunneling spectra of unconventional quasi-two-dimensional superconductors

L. Pisani [1,2] A. G. Moshe,[3,4] P. Pieri [1,2] G. Calvanese Strinati [5,6] and G. Deutscher[4]

[1]*Dipartimento di Fisica e Astronomia, Università di Bologna, 40127 Bologna, Italy*

[2]*INFN, Sezione di Bologna, 40127 Bologna, Italy*

[3]*National Institute of Chemical Physics and Biophysics, 12618 Tallinn, Estonia*

[4]*Raymond and Beverly Sackler School of Physics and Astronomy, Tel Aviv University, 6997801 Tel Aviv, Israel*

[5]*School of Science and Technology, Physics Division, Università di Camerino, 62032 Camerino, Italy*

[6]*CNR-INO, Istituto Nazionale di Ottica, Sede di Firenze, 50125 Firenze, Italy*

(Received 8 November 2023; revised 2 September 2024; accepted 12 September 2024; published 23 September 2024)

Superfluid condensation can fundamentally be different from that predicted by the Bardeen-Cooper-Schrieffer (BCS) theory. In a broad class of low-carrier-density superconductors, such as granular aluminum, doped nitrides, and high-T_c cuprates, tunneling experiments reveal strong rather than weak coupling, as well as a conductance that does not return to that of the normal state upon approaching the critical temperature T_c. Here, we show that this behavior is in quantitative agreement with a tunneling theory that takes into account the large pairing-fluctuation effects that occur in the crossover region from weak-coupling BCS to strong-coupling Bose-Einstein condensation, provided the coherence energy scale rather than the single-particle energy gap is used to evaluate the coupling ratio. We also propose that the tendency toward strong coupling is a generic property of quasi-2D low-carrier-density superconductors.

DOI: 10.1103/PhysRevB.110.L100506

Introduction. Lately, in condensed matter there has been an upsurge of interest in the Bardeen-Cooper-Schrieffer (BCS) to Bose-Einstein condensation (BEC) crossover owing to growing experimental evidence for its occurrence in iron-based materials [1], magic-angle twisted trilayer graphene [2], granular aluminum (grAl) [3], and high-T_c superconductors [4,5]. For a recent review, see Ref. [6]. These studies have followed the well-established achievements on the BCS-BEC crossover in ultracold Fermi gases obtained over the last twenty years [7].

In particular, in Ref. [4] a number of thermodynamic measurements on high-T_c cuprates have been organized in terms of the coupling ratio $2\Delta/k_BT_c$ (where Δ is the low-temperature gap parameter and k_B the Boltzmann constant), in such a way that the paired-fermion condensate was found to become optimally robust at the "magic gap ratio" $2\Delta/k_BT_c \approx 6$. In that work, the gap parameter was taken as the single-particle excitation energy $\Delta_{\rm p}$ obtained, for instance, from tunneling experiments. We wish to point out here that this choice is by no means obvious because in the cuprates there is an additional energy scale that characterizes the condensed state. This is the coherence energy scale $\Delta_{\rm c}$ obtained, for instance, from Andreev–Saint-James point contact spectroscopy [5]. We argue that this is actually the correct energy scale to be used to evaluate the coupling ratio $2\Delta/k_BT_c$, because this parameter is meant to characterize the condensed state. We show that if this choice is made, the tunneling conductance theory that we present is in good agreement with data from a variety of nonconventional superconductors, including (besides the cuprates) granular aluminum, Li-doped nitrides, and graphene, with values of the coupling ratio that do not exceed about 8. This implies that known unconventional superconductors are essentially all on the BCS side of the BCS-BEC crossover region, contrary to the conclusion reached in Ref. [4]. Examples about this important issue are given in Table I, where the values of $2\Delta/k_BT_c$ for $La_{2-x}Sr_xCuO_4$ obtained when using for Δ either $\Delta_{\rm c}$ or $\Delta_{\rm p}$ are compared. (Additional comparisons will be given in Fig. 4 below for the materials reported therein.) The link between the coupling ratio $2\Delta/k_BT_c$ and the coupling parameter $(k_Fa_F)^{-1}$, used to describe the BCS-to-BEC crossover in ultracold Fermi gases and utilized in our numerical calculations, is discussed in Supplemental Material [9].

In this Letter, we present a number of tunneling spectra taken in grAl under a variety of physical conditions and organize them in terms of the coupling ratio $2\Delta/k_BT_c$ as above specified. Our key finding is that the zero-bias conductance (ZBC) close to T_c decreases as the coupling factor increases. This pseudogap effect is already clearly observed at moderate values of the coupling ratio. It is not to be confused with the large pseudogap observed, for instance, in some underdoped cuprates. In addition, we also report data extracted from the literature for the zero-bias conductance close to T_c in Bi2212 and graphene. All these transport measurements are shown to compare favorably with theoretical calculations for the differential conductance, that take into account the effects of pairing fluctuations throughout the BCS-BEC crossover, provided the coherence energy scale $\Delta_{\rm c}$ is used to evaluate the coupling ratio. Our suggestion, for a crossover between weak-coupling BCS to strong-coupling BEC revealed in grAl and other quasi-2D unconventional superconductors, thus rests on the basis of a quantitative comparison between experimental and theoretical tunneling conductances. This comparison represents the main contribution of this work.

From our analysis we conclude that in condensed-matter samples the crossover region between BCS and BEC regimes

TABLE I. Values of $2\Delta/k_BT_c$, obtained when Δ is either Δ_c (from Andreev spectroscopy [8]) or Δ_p (from tunneling experiments [8]), for different x values of $La_{2-x}Sr_xCuO_4$ samples. (Asterisk (*) indicates value extrapolated from Fig. 3 of Ref. [8]).

x	Δ_c (meV)	Δ_p (meV)	T_c (K)	$2\Delta_c/k_BT_c$	$2\Delta_p/k_BT_c$
0.08	4.0		9.6	9.6	
0.10	6.5		25.3	6.0	
0.12	6.0		26.0	5.4	
0.13	8.0	18.0*	29.2	6.4	14
0.15	7.0	15.0	35.1	4.6	9.9
0.2	6.5	7.0	27.8	5.4	5.8

is essentially exhausted for $2\Delta/k_BT_c \lesssim 8$. We believe that the absence of condensed-matter samples with $2\Delta/k_BTc \gtrsim 8$, which would be far deep in the BEC regime of tightly bound pairs, is due to the charged nature of the fermions expected to pair up. In this respect, we will also point out that the quasi-2D nature of the materials here considered makes the values of $2\Delta/k_BT_c$ somewhat larger than those expected for strictly 3D materials [9] (an issue that was not considered in Ref. [4]).

Comparison between experiment and theory. The quantity to be calculated and compared with the experimental data is the differential conductance [3,39]

$$\frac{dI}{dV}(eV) = B\int_{-\infty}^{+\infty} dE\, N_s(E)\left[-\frac{\partial f_F(E+eV)}{\partial E}\right], \qquad (1)$$

where eV is the difference in the chemical potential across the superconducting-normal junction with an applied voltage V, $N_s(E)$ the quasiparticle density of states (DOS) at energy E, $f_F(E) = 1/(e^{E/k_BT}+1)$ the Fermi function at temperature T, and B a constant whose value we shall not be concerned with (and set equal to unity for simplicity). In the following, we shall not distinguish between energy E and frequency ω by setting $\hbar = 1$. The DOS function $N_s(\omega)$ in Eq. (1) can, in turn, be expressed in terms of the *single-particle spectral function* $A(\mathbf{k},\omega)$ by integrating it over the wave vector $\mathbf{k}$:

$$N_s(\omega) = \int \frac{d\mathbf{k}}{(2\pi)^3} A(\mathbf{k},\omega). \qquad (2)$$

Results for $A(\mathbf{k},\omega)$ in the superfluid phase, over the whole temperature range below T_c and throughout the BCS-BEC crossover, were first obtained in Ref. [14] in terms of a t-matrix approach, as an extension of an analogous approach in the normal phase above T_c [36]. Recently, a refined version of this t-matrix approach was implemented to include the Gorkov-Melik-Barkhudarov (GMB) correction [40] across the BCS-BEC crossover, both in the normal [15] and superfluid [16] phases. This extended GMB approach has resulted in quite accurate comparisons with the experimental data for ultracold Fermi gases across the BCS-BEC crossover, both for the gap parameter Δ_0 at low temperature [41] and the critical temperature [22]. Here, we shall rely on this extended GMB approach to obtain the required single-particle spectral function for various couplings and temperatures [42]. Our theoretical analysis for a *dynamical* quantity like the differential conductance (1) complements that utilized in Ref. [4] to compare with thermodynamic data, and is justified because for dynamical quantities the non-self-consistent t-matrix approach is expected to be more reliable than its fully self-consistent counterpart [43].

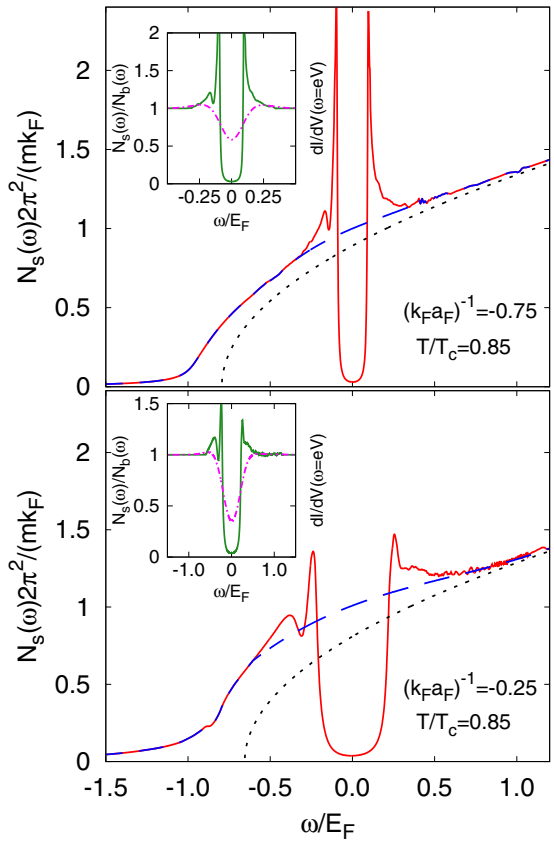

FIG. 1. DOS spectra $N_s(\omega)$ vs ω at $T = 0.85T_c$ for two different couplings in 3D (solid lines). In both panels, the noninteracting form $N_0(\omega) = m^{3/2}\sqrt{2(\omega+\mu)}/(2\pi^2)$ is shown for comparison (dotted lines), which corresponds to a noninteracting system with the value of the chemical potential μ of the interacting system for given coupling. Plots are normalized by $N_0(\omega=0) = mk_F/(2\pi^2)$ where we have set $\mu = E_F = k_F^2/(2m)$. Each panel also shows the associated background function $N_b(\omega)$ (dashed lines), obtained from the normalization procedure described in Ref. [9]. The insets report the ratio $N_s(\omega)/N_b(\omega)$ (solid lines) together with the corresponding normalized differential conductance (dash-dotted lines), obtained from Eq. (1) with $B = 1$ and $N_s(\omega)/N_b(\omega)$ replacing $N_s(\omega)$. (See Ref. [9] for further details.)

Theoretical results obtained for the DOS spectra $N_s(\omega)$ in 3D are shown in Fig. 1 at $T = 0.85T_c$ for two couplings on the BCS side of unitarity. In both cases, a dip is seen to occur in $N_s(\omega)$ about $\omega = 0$, accompanied by a two-peak structure which is more visible for negative ω. Like in Ref. [14], we associate the dip to a finite value of the thermodynamic gap parameter, and the two-peak structure to the presence of a pseudogap which develops upon approaching the normal phase. Both features become progressively more pronounced for increasing coupling. To highlight these features, in the insets of Fig. 1 the DOS spectra are normalized by the background function $N_b(\omega)$ described in Ref. [9], which aims at eliminating any irrelevant reference to the 3D background of the theoretical DOS spectra. This is achieved by taking $N_b(\omega)$

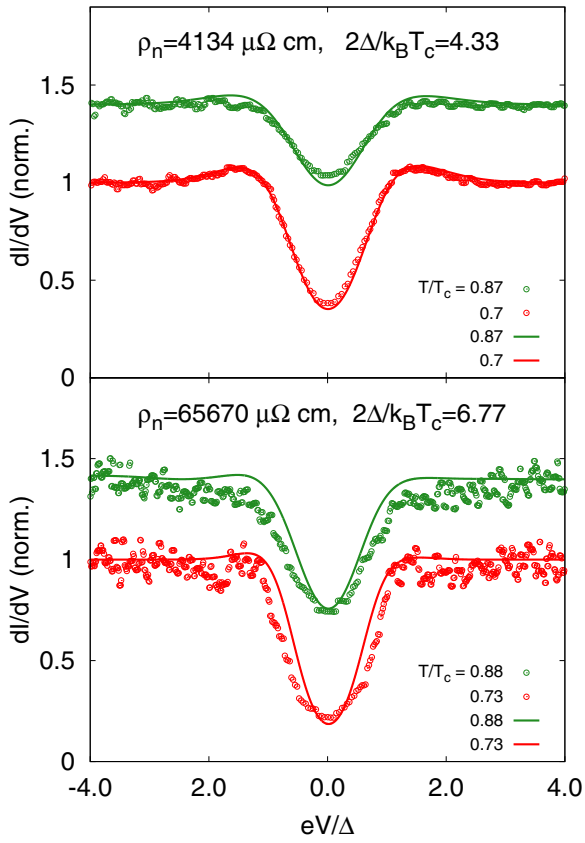

FIG. 2. Normalized differential conductance vs voltage for two characteristic measured samples, identified by their resistivity ρ_n and coupling ratio $2\Delta/k_BT_c$. Open circles are experimental data and solid lines are theoretical results calculated for the values $(k_Fa_F)^{-1} = (-0.75, -0.25)$ of the nominal coupling (from top to bottom). Experimental and theoretical data are compared with each other by normalizing the frequency by the respective values of the gap parameter Δ_0 at low temperature. Results for the larger temperatures are shifted upward for clarity. (See Ref. [9] for further details).

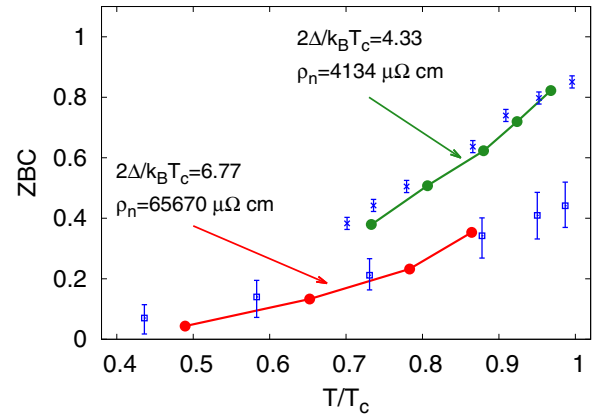

FIG. 3. Zero-bias conductance (ZBC) vs reduced temperature for the same samples of Fig. 2. Crosses and empty squares with error bars are experimental data, and filled circles are theoretical results obtained for the same values of the nominal coupling $(k_Fa_F)^{-1}$ of Fig. 2. In all cases, the temperature is in units of the respective value of the critical temperature T_c.

to coincide with $N_s(\omega)$ at large frequencies, where kinetic energy dominates over interaction, with a simple interpolation at low frequencies. This procedure enables us to extract in an effective way the quasi-2D character of the spectra, with the pseudogap associated with pairing fluctuations being regarded as a local quantity that should not appreciably differ in 3D and quasi-2D [31] (cf. also the discussion below and Ref. [9]). Further results for the temperature dependence of the DOS spectra at fixed coupling are reported in Ref. [9], where the persistence of the pseudogap upon approaching T_c is evident.

To draw a meaningful comparison between experiment and theory, the experimental differential conductance dI/dV spectra have been normalized by fitting the data in the range of $1.5 < |V| < 3.0$ mV to the form $dI/dV \propto |V|$ and then dividing the measured dI/dV by the extrapolated values obtained from the fit for $|V| < 3.0$ mV. The experimental differential conductances below T_c for two representative samples are shown in Fig. 2 at two selected temperatures, where they are plotted as a function of bias normalized by their respective zero-temperature gap Δ. The lower resistivity sample (with $T_c = 2.31$ K and $2\Delta/k_BT_c = 4.33$) appears to be close to the BCS side (upper panel), while the higher resistivity sample (with $T_c = 1.37$ K and $2\Delta/k_BT_c = 6.77$) to be close to the unitarity regime (lower panel), with the estimated value $\Delta/E_F \simeq 0.35$ [10,16]. In all cases, the experimental data are seen to closely match the overall theoretical trend, signaling further that the behavior of both considered samples deviates from what would be expected in the BCS weak-coupling limit. The procedure for associating to a given sample the nominal value of the coupling $(k_Fa_F)^{-1}$ is discussed in Ref. [9], where the quasi-2D character of the samples is taken into account in an effective way. Note how, for the differential conductance, the convolution with the derivative of the Fermi function in Eq. (1) smears out the two-peak structure of Fig. 1 for $N_s(\omega)$. Note further that, by comparing tunnel and optical gaps, in Ref. [3] we concluded that atomic disorder effects are negligible in grAl. This excludes disorder effects [44] as an explanation for the pseudogap observed in grAl.

A further measurable quantity of interest is the zero-bias conductance (ZBC), obtained as the limit $dI/dV|_{V\to 0}$. Figure 3 shows the dependence of ZBC on temperature for the same samples of Fig. 2. (For the higher ρ_n, the ZBC value extrapolated to $T = 0$ from the measured ones has been subtracted off to avoid spurious (leakage) effects at the contacts. Additional spurious effects, possibly arising from the formation of pinholes in the Al oxide barrier layer, are minimized by our oxidization procedure [3]). The corresponding theoretical dependence, calculated for the same nominal couplings of Fig. 2, is seen to follow the same trend as the experiment. For the higher ρ_n, note the strong depletion of ZBC for both experiment and theory, which extrapolates to a value less than 0.5 upon approaching T_c. For the lower ρ_n, this extrapolation gets instead close to unity, a value which is expected to be reached in the BCS limit of the BCS-BEC crossover.

Finally, Fig. 4 shows the experimental values for ZBC versus the coupling ratio $2\Delta/k_BT_c$ for several samples at $T = 0.85T_c$, together with the corresponding theoretical results also at $T = 0.85T_c$. In this way, we avoid entering the critical region close to T_c, where the theory would need to

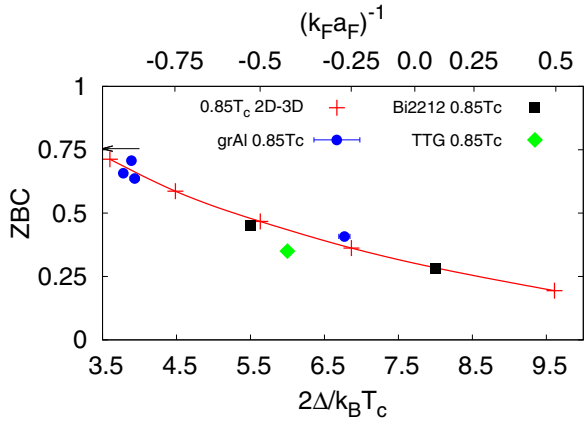

FIG. 4. ZBC vs coupling ratio. The dependence of the zero-bias conductance (ZBC) on the coupling ratio $2\Delta/k_BT_c$ for grAl at $0.85T_c$ (filled circles) is compared with the theoretical results obtained by the extended GMB approach also at $0.85T_c$ (crosses and solid line). Further experimental values are shown for Bi2212 (filled squares) (from Ref. [45]) and for twisted trilayer graphene (filled diamond) (from Ref. [13]), both at $0.85T_c$. The arrow signals the BCS mean-field result at $0.85T_c$ for coupling $(k_Fa_F)^{-1} = -1.5$. The upper horizontal axis reports the values of the nominal coupling $(k_Fa_F)^{-1}$ associated with the values of the coupling ratio $2\Delta/k_BT_c$ according to the procedure summarized in Fig. 5 of Ref. [9].

be refined by including additional fluctuation corrections [9]. This critical region is larger at unitarity than in the BCS regime [21], as implicitly confirmed by the different extensions toward T_c of the theoretical results reported in Fig. 3 for the two samples. One sees from Fig. 4 that the ZBC decreases as the coupling ratio increases in good agreement with the theoretical trend, being reduced by about half when reaching $2\Delta/k_BT_c \simeq 6$. Figure 4 also shows that the above overall trend is not unique to grAl by considering ZBC values for two other compounds, Bi2212 [45] and twisted trilayer graphene (TTG) [13]. For both of them the tunneling gap is substantially larger than the coherence energy scale obtained by point contact spectroscopy, such that for TTG $2\Delta_c/k_BT_c = 6$ while $2\Delta_p/k_BT_c = 15$–19, for underdoped Bi2212 $2\Delta_c/k_BT_c = 8$ while $2\Delta_p/k_BT_c = 10$, and for overdoped Bi2212 $2\Delta_c/k_BT_c = 5.5$ while $2\Delta_p/k_BT_c = 8.7$. Good agreement with theory is only obtained if the Δ_c is used to evaluate the coupling ratio. On the other hand, Table I suggests that for our grAl samples, for which the coupling ratio as measured by tunneling does not exceed 7, differences between Δ_p and Δ_c should be minor. We further note that, besides Bi2212 and TTG, grAl is also a quasi-2D superconductor [46]. In this respect, one should mention that, away from the weak-coupling (BCS) regime, the values of the coupling ratio $2\Delta/k_BT_c$ change appreciably when calculated in 3D or in the strictly 2D case of a Berezinskii-Kosterlitz-Thouless transition. This change is here taken into account when associating the experimental value of $2\Delta/k_BT_c$ with the nominal coupling $(k_Fa_F)^{-1}$ used for theoretical calculations [9].

We note that when the proper energy scale is used to evaluate the coupling ratio, this ratio never exceeds the value of about 8 which corresponds to the unitary limit, suggesting that this is a universal property of quasi-2D superconductors close to a Mott transition, triggered by Coulomb interaction.

Discussion and outlook. The extensive comparison we have presented of the experimental and theoretical spectra for the differential conductance is made between experimental samples (like grAl films) that are quasi-2D systems and theoretical calculations that are performed for a 3D system. However, there is intrinsically no contradiction in making this comparison, inasmuch as the experiment seems to have access to a pseudogap phase related to pairing fluctuations which survive across T_c. On physical grounds, what should, in fact, be important is the *local* behavior of pairing correlations occurring inside a Cooper pair (or, at most, among nearby Cooper pairs). Under these circumstances, pseudogap phenomena occurring in a fermionic superfluid should be envisaged as due to persistency of "local-pairing order" across T_c, that survives even when (off-diagonal) long-range order is lost. Accordingly, one expects that there should not be too much of a difference between 3D and quasi-2D calculations for this local property. In this context, one should mention a recent experimental work [31] where it was shown that dimensionality has only limited influence on the stability of strongly interacting fermionic superfluids, in the sense that there is nothing significantly new in the superfluid properties of 3D and 2D Fermi superfluids.

These arguments are reinforced by the theoretical work of Ref. [47] where the effect of a weak interlayer coupling on BE condensates was studied, with the result that a small interlayer coupling was found sufficient to preserve BEC with an only slightly reduced condensation temperature, as well as by the analogy with a layered antiferromagnet mentioned in Ref. [9], where local antiferromagnetic correlations surviving above the Néel temperature were also seen not to markedly depend on the ratio between the intra- and interlayer couplings. In all cases, local correlations do eventually allow achieving symmetry breaking at a slightly reduced temperature.

Our results corroborate the mounting experimental evidence that a combination of small carrier density and reduced dimensionality acts to favor superconductivity [48]. This is the case for systems as diverse as the high-T_c cuprates, grAl, and twisted trilayer graphene. Nitrides such as Li_xHfNCl were not considered in Fig. 4 because their coherence energy scale has not been reported so far, but the same combination holds for them too. One is thus led to look for a general (yet simple) argument to explain these observations. This argument may be provided by the jellium model for superconductivity [49–51]. In this model, the electron-electron attraction V increases as the carrier density decreases. In 3D this increase is counterbalanced by a reduced density of states, so that the BCS parameter N_0V and the critical temperature get eventually reduced for decreasing carrier density. This is not the case in 2D when the density of states remains constant, such that both N_0V and V should increase for reduced carrier density. As a consequence, the interaction parameter V might be strong enough to promote a crossover from BCS to BEC. There are, however, a few problems with this argument. In 2D localization sets in even for extremely small disorder and might prevent superfluidity. In addition, BEC does not occur in strictly 2D at finite temperature. These difficulties are in principle removed by the quasi-2D approach.

Conclusions. The detailed experimental tunneling results on quasi-2D grAl, Bi2212, and twisted trilayer graphene presented in this work appear to exhibit the main features expected for a BCS-BEC crossover—namely, a coupling ratio $2\Delta/k_BT_c$ that evolves continuously from the weak-coupling (BCS) limit value to larger values typical of the crossover regime, and at the same time monotonically decreasing values of zero-bias conductance close to T_c with increasing coupling ratio. We have further shown that for three families of small-carrier-density quasi-2D systems here considered, there appears to be a universal correlation between the coupling ratio and the zero-bias conductance, and that this correlation is in agreement with theoretical results obtained for the BCS-BEC crossover provided the coherence energy scale is used to evaluate the coupling ratio.

Acknowledgement. A.G.M. acknowledges support by the Estonian Research Council under Grant No. MOBJD1103.

[1] Y. Lubashevsky, E. Lahoud, K. Chashka, D. Podolsky, and A. Kanigel, Shallow pockets and very strong coupling superconductivity in $FeSe_xTe_{1-x}$, Nat. Phys. **8**, 309 (2012).

[2] J. M. Park, Y. Cao, K. Watanabe, T. Taniguchi, and P. Jarillo-Herrero, Tunable strongly coupled superconductivity in magic-angle twisted trilayer graphene, Nature (London) **590**, 249 (2021).

[3] A. Glezer Moshe, G. Tuvia, S. Avraham, E. Farber, and G. Deutscher, Tunneling study in granular aluminum near the Mott metal-to-insulator transition, Phys. Rev. B **104**, 054508 (2021).

[4] N. Harrison and M. K. Chan, Magic gap ratio for optimally robust fermionic condensation and its implications for high-T_c superconductivity, Phys. Rev. Lett. **129**, 017001 (2022).

[5] G. Deutscher, Coherence and single-particle excitations in the high-temperature superconductors, Nature (London) **397**, 410 (1999).

[6] Q. Chen, Z. Wang, R. Boyack, S. Yang, and K. Levin, When superconductivity crosses over from BCS to BEC, Rev. Mod. Phys. **96**, 025002 (2024).

[7] G. Calvanese Strinati, P. Pieri, G. Röpke, P. Schuck, and M. Urban, The BCS-BEC crossover: From ultra-cold Fermi gases to nuclear systems, Phys. Rep. **738**, 1 (2018).

[8] R. S. Gonnelli, A. Calzolari, D. Daghero, L. Natale, G. A. Ummarino, V. A. Stepanov, and M. Ferretti, Doping dependence of the superconducting gap by Andreev reflection in $Au/La_{2-x}Sr_xCuO_4$ point-contact junctions, J. Phys. Chem. Solids **63**, 2369 (2002).

[9] See Supplemental Material at http://link.aps.org/supplemental/10.1103/PhysRevB.110.L100506 for details on (i) experimental methods; (ii) the relation between the coupling parameter $(k_Fa_F)^{-1}$ and the coupling ratio $2\Delta/k_BT_c$; (iii) the normalization procedure of the DOS spectra; (iv) the emergence of a critical region upon approaching T_c; (v) the issue of a meaningful comparison between the 3D and 2D values of the coupling ratio $2\Delta/k_BT_c$; (vi) an analogy with the dimensional crossover occurring in a layered antiferromagnet; (vii) the coupling dependence of the low-temperature coherence length which also includes Refs. [2–4,7,10–38].

[10] A. G. Moshe, E. Farber, and G. Deutscher, Optical conductivity of granular aluminum films near the Mott metal-to-insulator transition, Phys. Rev. B **99**, 224503 (2019).

[11] C. Renner and Ø. Fischer, Vacuum tunneling spectroscopy and asymmetric density of states of $Bi_2Sr_2CaCu_2O_{8+\delta}$, Phys. Rev. B **51**, 9208 (1995).

[12] Ø. Fischer, M. Kugler, I. Maggio-Aprile, and C. Berthod, Scanning tunneling spectroscopy of high-temperature superconductors, Rev. Mod. Phys. **79**, 353 (2007).

[13] H. Kim, Y. Choi, C. Lewandowski, A. Thomson, Y. Zhang, R. Polski, K. Watanabe, T. Taniguchi, J. Alicea, and S. Nadj-Perge, Evidence for unconventional superconductivity in twisted trilayer graphene, Nature (London) **606**, 494 (2022).

[14] P. Pieri, L. Pisani, and G. C. Strinati, BCS-BEC crossover at finite temperature in the broken-symmetry phase, Phys. Rev. B **70**, 094508 (2004).

[15] L. Pisani, A. Perali, P. Pieri, and G. C. Strinati, Entanglement between pairing and screening in the Gorkov-Melik-Barkhudarov correction to the critical temperature throughout the BCS-BEC crossover, Phys. Rev. B **97**, 014528 (2018).

[16] L. Pisani, P. Pieri, and G. C. Strinati, Gap equation with pairing correlations beyond the mean-field approximation and its equivalence to a Hugenholtz-Pines condition for fermion pairs, Phys. Rev. B **98**, 104507 (2018).

[17] G. D. Mahan, *Many-Particle Physics* (Kluwer, New York, 2000).

[18] A. Larkin and A. Varlamov, *Theory of Fluctuations in Superconductors* (Oxford University Press, Oxford, 2009).

[19] V. V. Dorin, R. A. Klemm, A. A. Varlamov, A. I. Buzdin, and D. V. Livanov, Fluctuation conductivity of layered superconductors in a perpendicular magnetic field, Phys. Rev. B **48**, 12951 (1993).

[20] R. Haussmann, W. Rantner, S. Cerrito, and W. Zwerger, Thermodynamics of the BCS-BEC crossover, Phys. Rev. A **75**, 023610 (2007).

[21] E. Taylor, Critical behavior in trapped strongly interacting Fermi gases, Phys. Rev. A **80**, 023612 (2009).

[22] M. Link, K. Gao, A. Kell, M. Breyer, D. Eberz, B. Rauf, and M. Köhl, Machine learning the phase diagram of a strongly interacting Fermi gas, Phys. Rev. Lett. **130**, 203401 (2023).

[23] E. Vitali, H. Shi, M. Qin, and S. Zhang, Visualizing the BEC-BCS crossover in a two-dimensional Fermi gas: Pairing gaps and dynamical response functions from *ab initio* computations, Phys. Rev. A **96**, 061601(R) (2017).

[24] Y.-Y. He, H. Shi, and S. Zhang, Precision many-body study of the Berezinskii-Kosterlitz-Thouless transition and temperature-dependent properties in the two-dimensional Fermi gas, Phys. Rev. Lett. **129**, 076403 (2022).

[25] M. Feld, B. Fröhlich, E. Vogt, M. Koschorreck, and M. Köhl, Observation of a pairing pseudogap in a two-dimensional Fermi gas, Nature (London) **480**, 75 (2011).

[26] V. Pietilä, Pairing and radio-frequency spectroscopy in two-dimensional Fermi gases, Phys. Rev. A **86**, 023608 (2012).

[27] F. Marsiglio, P. Pieri, A. Perali, F. Palestini, and G. C. Strinati, Pairing effects in the normal phase of a two-dimensional Fermi gas, Phys. Rev. B **91**, 054509 (2015).

[28] F. Pistolesi and G. C. Strinati, Evolution from BCS superconductivity to Bose condensation: Role of the parameter $k_F\xi$, Phys. Rev. B **49**, 6356 (1994).

[29] M. Randeria, J. M. Duan, and L. Y. Shieh, Superconductivity in a two-dimensional Fermi gas: Evolution from Cooper pairing to Bose condensation, Phys. Rev. B **41**, 327 (1990).

[30] M. Marini, F. Pistolesi, and G. Calvanese Strinati, Evolution from BCS superconductivity to Bose condensation: Analytic results for the crossover in three dimensions, Eur. Phys. J. B **1**, 151 (1998).

[31] L. Sobirey, H. Biss, N. Luick, M. Bohlen, H. Moritz, and T. Lompe, Observing the influence of reduced dimensionality on fermionic superfluids, Phys. Rev. Lett. **129**, 083601 (2022).

[32] F. Palestini and G. C. Strinati, Systematic investigation of the effects of disorder at the lowest order throughout the BCS-BEC crossover, Phys. Rev. B **88**, 174504 (2013).

[33] N. Majlis, S. Selzer, and G. C. Strinati, Dimensional crossover in the magnetic properties of highly anisotropic antiferromagnets, Phys. Rev. B **45**, 7872 (1992).

[34] N. Majlis, S. Selzer, and G. C. Strinati, Dimensional crossover in the magnetic properties of highly anisotropic antiferromagnets. II. Paramagnetic phase, Phys. Rev. B **48**, 957 (1993).

[35] H. A. Mook, J. W. Lynn, and R. M. Nicklow, Temperature dependence of the magnetic excitations in nickel, Phys. Rev. Lett. **30**, 556 (1973).

[36] A. Perali, P. Pieri, G. C. Strinati, and C. Castellani, Pseudogap and spectral function from superconducting fluctuations to the bosonic limit, Phys. Rev. B **66**, 024510 (2002).

[37] F. Pistolesi and G. C. Strinati, Evolution from BCS superconductivity to Bose condensation: Calculation of the zero-temperature phase coherence length, Phys. Rev. B **53**, 15168 (1996).

[38] A. Glezer Moshe, E. Farber, and G. Deutscher, From orbital to Pauli-limited critical fields in granular aluminum films, Phys. Rev. Res. **2**, 043354 (2020).

[39] M. Tinkham, *Introduction to Superconductivity* (R. E. Krieger, Malabar, 1980).

[40] L. P. Gor'kov and T. M. Melik-Barkhudarov, Contribution to the theory of superfluidity in an imperfect Fermi gas, Sov. Phys. JETP **13**, 1018 (1961) [Zh. Eksp. Teor. Fiz. **40**, 1452 (1961)].

[41] H. Biss, L. Sobirey, N. Luick, M. Bohlen, J. J. Kinnunen, G. M. Bruun, T. Lompe, and H. Moritz, Excitation spectrum and superfluid gap of an ultracold Fermi gas, Phys. Rev. Lett. **128**, 100401 (2022).

[42] Inclusion of the GMB correction does not modify the procedure of analytic continuation from imaginary Matsubara frequencies $i\Omega_\nu$ to real frequencies ω, used in the t-matrix approach of Ref. [14] to obtain the single-particle spectral function $A(\mathbf{k}, \omega)$, because here like in Ref. [16] the GMB correction is considered only in the static limit.

[43] M. Pini, P. Pieri, and G. C. Strinati, Fermi gas throughout the BCS-BEC crossover: Comparative study of t-matrix approaches with various degrees of self-consistency, Phys. Rev. B **99**, 094502 (2019).

[44] B. L. Altshuler, A. G. Aronov, and P. A. Lee, Interaction effects in disordered Fermi systems in two dimensions, Phys. Rev. Lett. **44**, 1288 (1980).

[45] V. M. Krasnov, Temperature dependence of the bulk energy gap in underdoped $Bi_2Sr_2CaCu_2O_{8+\delta}$: Evidence for the mean-field superconducting transition, Phys. Rev. B **79**, 214510 (2009).

[46] G. Deutscher and S. A. Dodds, Critical-field anisotropy and fluctuation conductivity in granular aluminum films, Phys. Rev. B **16**, 3936 (1977).

[47] K. K. Witkowski and T. K. Kopeć, Dimensional crossover in the Bose-Einstein condensation confined to anisotropic three-dimensional lattices, J. Low Temp. Phys. **201**, 340 (2020).

[48] D. Qiu, C. Gong, S. Wang, M. Zhang, C. Yang, X. Wang, and J. Xiong, Recent advances in 2D superconductors, Adv. Mater. **33**, 2006124 (2021).

[49] P. Nozières and D. Pines, Electron interaction in solids. General formulation, Phys. Rev. **109**, 741 (1958).

[50] P. G. de Gennes, *Superconductivity of Metals and Alloys* (Westview Press, Boulder, 1999), Chap. 4.

[51] G. Deutscher, *New Superconductors: From Granular to High T_c* (World Scientific, Singapore, 2006), Chap. 4.